Turbulent flow pressure loss due to a design obstruction within small-scale channel

Mirza Popovac[1], Alois Steiner[2], Rainer Sonnenberger[3]

[1]*Austrian Institute of Technology, Vienna, Austria. mirza.popovac@ait.ac.at (corresponding author)*

[2]*Virtual Vehicle Research GmbH, Graz, Austria. alois.steiner@v2c2.at (co-author)*

[3]*Valeo Klimasysteme GmbH, Bad Rodach, Germany. rainer.sonnenberger@valeo.com (co-author)*

Abstract

This paper presents the results of the numerical analysis of the turbulent flow within a plane channel with a protruding element mounted near the bottom wall. As the outcome of this analysis, the correlation between the pressure loss and the position of the protrusion is obtained, and compared with the empirical expression for the pressure drop within the horizontal pipe caused by the sudden contraction.

Introduction

The general trend of miniaturization in the engineering components brings new challenges for the small-scale designs, as in the case of the flow distribution systems where protruding elements which due to its small-scale design (the size in the range of millimeters) and the requirements for their simplicity and low price manufacturing have very low stiffness, bringing them to the limit of being bended inwards to the flow during the operation. Obviously, such eventuality would cause the pressure loss increase in the flow distribution system, and potentially lead to the malfunctioning of the entire system. An example of this behavior is shown in Figure 1, where the numerical analysis of the system involving the evaporator showed how the flow distribution malfunctioning can cause the inactive area of the evaporator to significantly increase (red zone).

In order to quantify the influence of a general design obstruction on the pressure loss within a small-scale channel, this paper is presenting the results of the computational fluid dynamics (CFD) analysis of the turbulent flow within a plane channel: in order to simplify the geometrical representation of a protruding element, a straight flap with rounded edges was placed near the bottom wall of the channel (as sketched

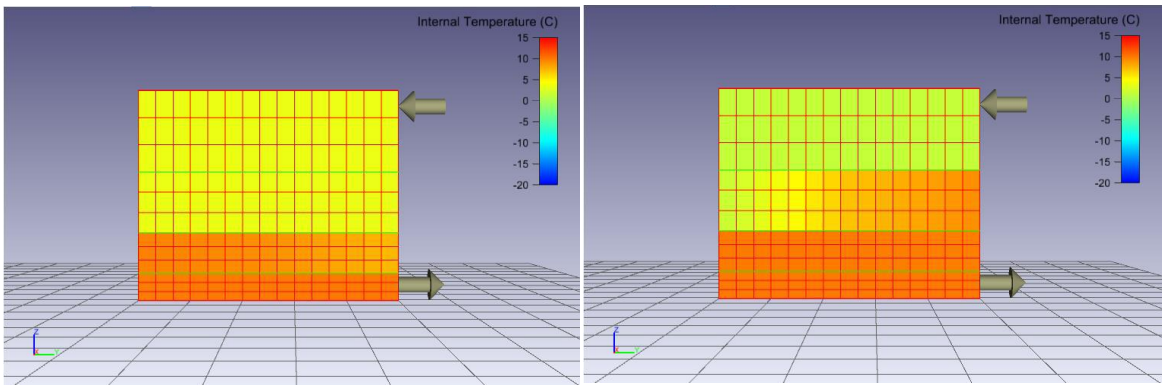

Figure 1: internal temperature of the evaporator connected to a fluid distribution system with variable pressure loss, indicating correspondingly high (left) and low (right) portion of the evaporator active area.

in Figure 2), and different levels of protrusions were modeled by varying the flap angle. With the constant velocity imposed on the inlet section of the channel, the outcome of this numerical analysis is the correlation between the pressure drop within the channel (defined as the pressure difference between the inlet and outlet section of the channel) and the flap position. The obtained correlation is compared with the empirical expression for the pressure loss within the horizontal pipe caused by its sudden contraction, and the analysis is concluded with the discussion of the main findings.

Setup

This CFD analysis was performed with OpenFoam-v1906, using steady-state incompressible isothermal turbulent solver simpleFoam. The mesh was generated with snappyHexMesh (Figure 2), featuring boundary layer cells around the flap and different levels of cell refinement based on the distance from the flap. The channel height was 6 mm, the flap length and thickness were 5.6 mm and 0.1 mm respectively, with six flap lengths distance both to the inlet and outlet of the channel. A-posteriori check gave y^+ values in the range between 0.6 and 7.8 for all simulated cases. As the analyzed case is two-dimensional, in order to allow for the flow leakages from a real case, small rectangular block was placed onto the bottom at a small distance from the flap origin. In the same regard, the flap angle α was varied (with the 5° incremental steps) between 5° and 85°, and the entire analysis has been executed through an automated script.

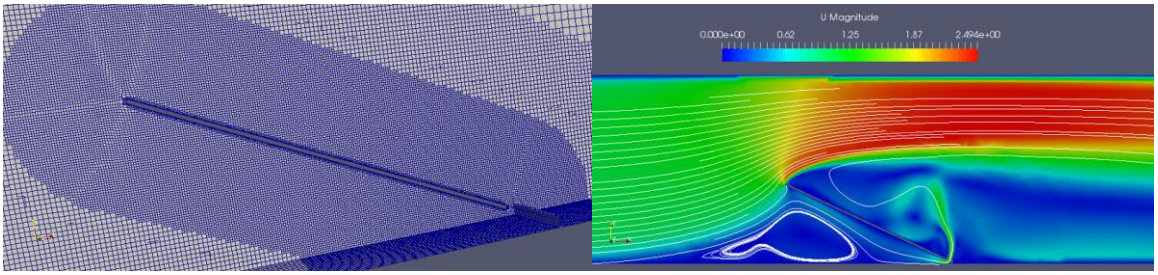

Figure 2: numerical mesh around the flap (left) sketching the geometry, and the velocity magnitude with streamlines in the vertical mid-plane (right) depicting the characteristic flow pattern.

The operating flow conditions were imposed through the fixed inlet values for the velocity (*v=1 m/s*) and turbulence quantities (assuming fully developed turbulent profile, imposed through the turbulent intensity and mixing length), and free outlet with zero-value fixed pressure, while the symmetry was imposed on the sides. All walls were treated as non-moving, with no-slip boundary condition. To test the influence of the turbulent effects, the k-omega SST and k-epsilon RNG model of turbulence were deployed in the simulations. The kinematic viscosity of water ν*=0.8E-6 m²/s* was taken for the simulations. For the pressure equation GAMG solver was used, and the smooth solver for all other equations, while for their respective under-relaxation factors the values 0.3 and 0.7 were taken.

Results

For this two-dimensional case, the view of the overall flow pattern is obtained from the velocity magnitude distribution (complemented with the streamlines) over the vertical mid-plane, as shown in Figure 2 for a selected flap angle. The resulting flow features a strong deflection at the upstream rounded edge of the flap, after which the flow separates and subsequently re-attaches at the top surface of the flap (whereby the size of the separation on the flap surface depends on the geometry and the flow conditions). Under the bottom surface of the flap a recirculation bubble is established, after which a part of the stream 'leaks' between the flap origin and the rectangular box and influences the flow at the downstream side of the flap. Past the flap, the flow recovers in the form which depends on the flap angle.

Although the analyzed case does not correspond fully to the pipe sudden contraction, there is a similarity with the flow pattern characteristic for the flow past the flap. Therefore, the calculated pressure loss was compared with the Borda-Carnot equation for the pressure drop within the horizontal pipe caused by the sudden contraction [1]. In this empirical correlation the usual loss coefficient is expressed in terms of ratios of the geometrical features – the area of the incoming flow section A, the smallest section of separation contraction A_s, and the final section after contraction A_c (Figure 3):

$$\frac{\Delta P}{\rho} = \frac{1}{2}\left(1 - \frac{1}{\mu}\right)^2 v^2 \left(\frac{A}{A_c}\right)^2 \qquad (1)$$

with v and ρ being the bulk velocity and density respectively, the static pressure P being recast into the kinematic pressure $p=P/\rho$ (which is the solved flow quantity in simpleFoam, following the constant density assumption), and the coefficient of the separation contraction $\mu=A_s/A_c$ is approximated as [2]:

$$\mu = 0.63 + 0.37\left(\frac{A_c}{A}\right)^3 \qquad (2)$$

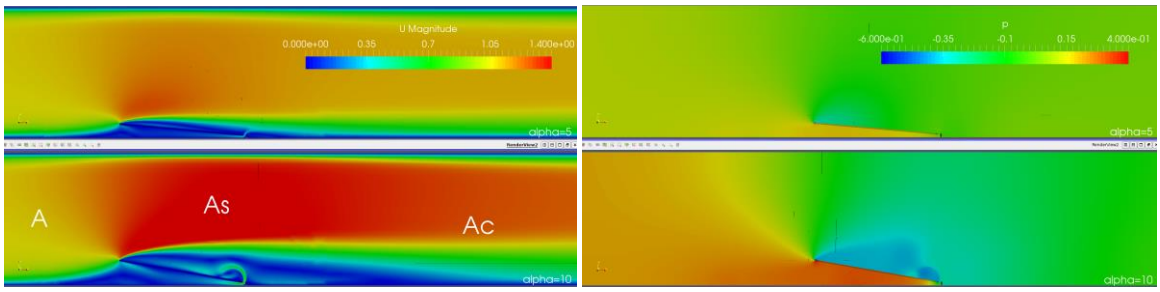

Figure 3: velocity magnitude (left) and the pressure distribution (right) over the vertical mid-plane for low flap angles (α=5° and α=10° top to bottom).

The pressure loss given with Eq.(1) is a function of the ratio between the flow sections before and after contraction. Here becomes obvious the main difference between the sudden pipe contraction and the present case, that the final contraction section A_c is not strictly defined here, but only indicted by the portion of the recovering stream (as denoted in Figure 3). Still, it can be related to the position of the flap:

$$\frac{A_c}{A} = (1 - \sin\alpha)^m \tag{3}$$

where the mounting height of the flap origin was neglected, and the exponent *m* was introduced to account for the difference between the geometric contraction and the flow contraction section.

As indicated in Figure 3, for low flap angles one can follow the development of the contraction from *A* to A_c (including the separation contraction A_s) similarly to the sudden pipe contraction. Since the contraction section is not strictly defined through the channel geometry (unlike in the pipe contraction case), in the present work its exact size is calibrated through a model parameter *m=1.5* in order to reduce the effect of the flow recovery (since it is leading to the spreading of the stream). Shown in Figure 4 for high flap angles, however, the region upstream of the flap starts to behave like the stagnation zone: the fluid stream is forced through the gap between the flap and the channel wall, creating a massive separation behind the flap which renders the concept of contraction areas invalid for this range of α.

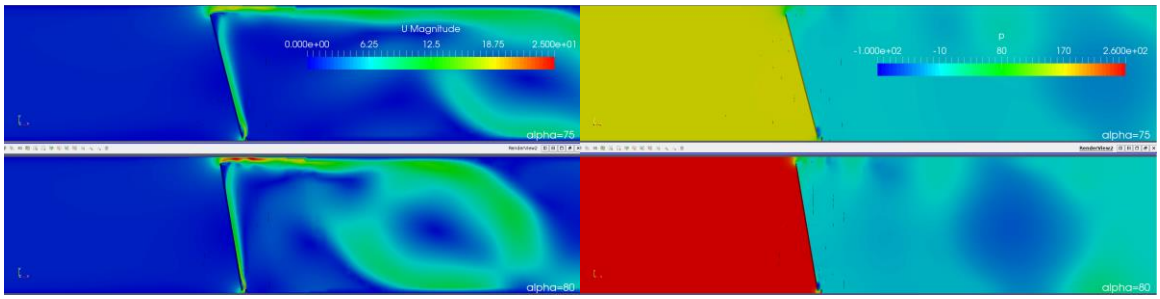

Figure 4: velocity magnitude (left) and the pressure distribution (right) over the vertical mid-plane for high flap angles (α=75° and α=80° top to bottom).

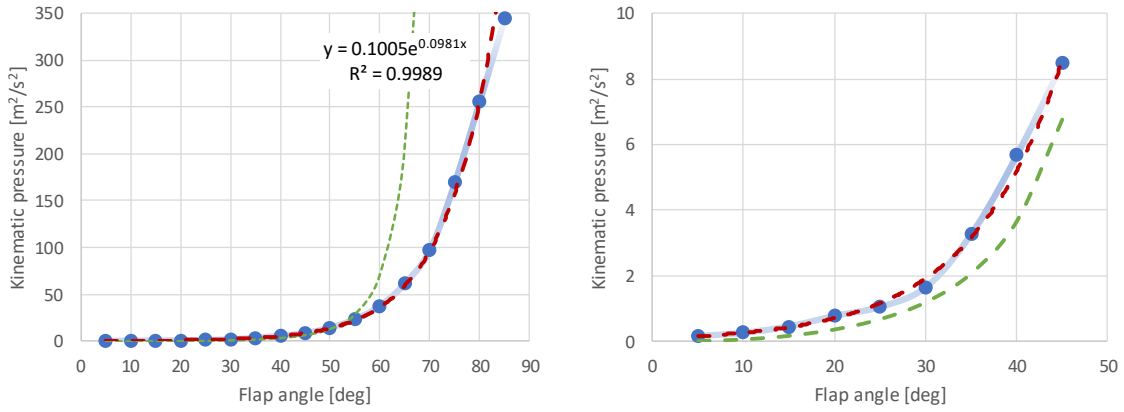

Figure 5: comparison between the calculated pressure losses (blue dot-line), the exponential function fitting (red dashed line) and the calibrated Borda-Carnot expression (green dashed line) for the entire flap angle variation (left) and only for the small angles (right).

To quantify the proposed pressure loss model, the calculated pressure drops from the individual flap valves are plotted in Figure 5 (blue). The exponential function fitting of the obtained results yields a very good approximation (red). The Borda-Carnot equation, with Eqs. (2) and (3) introduced as proposed, can produce the accuracy of approximately 10% for the flap angles lower than 45° (green), but fails completely above that threshold.

Conclusions

The mechanism recognized through the Borda-Carnot equation for the pressure drop within a sudden pipe contraction can be applied to relatively small obstructions within small-scale channels, though with the definition of the contraction section which is accounting for the effect of the flow recovery. As the obstruction size increases, the proposed contraction section characterization loses its validity, and the predicted exponential growth of the pressure drop cannot be recovered with such a simple formulation.

Acknowledgment

The presented work has been financially supported through the EU Programme Horizon 2020, Project SELFIE (Grant Agreement number: 824290).

References

(1) Batchelor, G. K. (1967), *An Introduction to Fluid Dynamics*, Cambridge University Press, ISBN 978-0-521-66396-0.

(2) Ortel, H.; Prandtl, L.; Böhle, M.; Mayes, K. (2004), *Prandtl's Essentials of Fluid Mechanics*, Springer, ISBN 978-0-387-40437-0.